Effective computer simulation of strongly coupled Coulomb fluids

Effective computer simulation of strongly coupled Coulomb fluids

E S Yakub

Computer Science Department, Odessa State Economic University, Preobrazhenskaya 8, 65026, Odessa, Ukraine

E-mail: yakub@unive.odessa.ua

Abstract
The problem of accurately accounting for long ranged Coulomb forces within periodic boundaries in Monte Carlo and molecular dynamics computer simulation of strongly coupled Coulomb systems is considered. Periodicity artefacts characteristic of the conventional Ewald summation procedure are eliminated by angular averaging of Ewald sums over all orientations of the main cell. This approach provides an effective analytical electrostatic interaction potential and allows fast and accurate simulations of strongly coupled Coulomb fluids even on a modern PC. The effectiveness and accuracy of the method is illustrated on simple non-ideal plasma models.

PACS numbers: 07.05.Tp, 52.65.−y

1. Introduction

Despite great progress achieved in the microscopic description of condensed matter since the pioneering works of Madelung [1] and Ewald [2], correct description of long ranged Coulomb forces under conditions of computer simulation with periodic boundary conditions (PBC) still remains a topical issue both in conventional [3] and *ab initio* [4] computer simulations. The standard Ewald procedure [5] when applied to Coulomb systems under PBC invokes a non-isotropic electric field having cubic symmetry of a crystalline lattice composed of main Monte Carlo (MC) or molecular dynamics (MD) computation cells as elementary units. It results in an artificial 'crystalline field' in simulations of fluids, amorphous solids and other spatially uniform condensed phases. An example presented in [6] shows how important these periodicity artefacts may be in real simulations.

In *ab initio* computer simulations [7], the number of particles in the main cell is very limited, mainly by the supercomputer facilities available. Periodicity artefacts imposed by the conventional Ewald summation procedure may appear a major issue here. Being almost negligible at small distances even for a relatively small number N of charged particles in the

cell, these artefacts become important at larger distances. For instance, for $N = 200$, which is characteristic for up-to-date *ab initio* simulations using the best available computing codes and facilities [8, 9], the maximum value of the Ewald artefact is about 10% in effective Coulomb interaction energy at a distance of third coordination sphere and reaches $\sim$100% at the edge of the main cell [6].

Accurate computer simulations of biochemical and other systems having complex elemental composition require sometimes up to a million particles [10] in the main cell. Obviously, the larger the number of charged particles in the main cell, the more acute is the problem of the effective evaluation of the electrostatic contribution. Periodicity artefacts in this case are small but the heavy processor load imposed by the conventional Ewald summation procedure is crucial in such simulations. Thus, the problem of effective and accurate evaluation of electrostatic fields is important for any size of the cell.

An approach eliminating these periodicity artefacts in spatially uniform Coulomb systems and cardinally increasing efficiency of simulation was proposed recently [6]. This approach is outlined in section 2, in section 3 its generalization on a one-component plasma (OCP) and a semi-classical model of hydrogen plasma, as well as new MC and MD simulation results, demonstrating the accuracy of the method, are presented, in section 4 these results and the possibility of other applications of the method are discussed.

2. Pre-averaged effective potentials

Let us consider a standard cubic main cell of edge L and volume $V = L^3$, containing $N = \sum_{\alpha=1}^{M} N_\alpha$ charged particles of M sorts within PBC. The electrostatic forces acting between the ith and the jth particles obey the Coulomb law:

$$F_{ij} = \frac{Q_i Q_j}{4\pi \varepsilon_0 r_{ij}^2}.$$

Here, $r_{ij} = |\mathbf{r}_i - \mathbf{r}_j|$ is the distance between the ith and jth charged particles and Q_i is the value of the ith point charge of type α: $Q^{(\alpha)} = \{Q^{(1)}, \ldots, Q^{(M)}\}$. We shall here assume that the electro-neutrality condition

$$\sum_{i=1}^{N} Q_i = \sum_{\alpha=1}^{M} N_\alpha Q^{(\alpha)} = 0 \tag{1}$$

is satisfied, and the standard PBC are imposed as described in [3, 5]. The total Coulomb energy of N charges in the main cell is

$$U_N^{(C)} = \sum_{1 \leqslant i \leqslant N} Q_i \varphi(\mathbf{r}_i),$$

where $\varphi(\mathbf{r}_i)$ is the electrostatic potential at the position $\mathbf{r}_i$ of the ith charge. According to the conventional Ewald scheme [5], this contribution is in turn the sum of one- and two-particle terms:

$$\varphi(\mathbf{r}_i) = \varphi_1(\mathbf{r}_i) + \frac{1}{2}\sum_{\substack{j \neq i}}^{N} \varphi_2(\mathbf{r}_i, \mathbf{r}_j).$$

In the absence of external fields, the unitary potential is a constant:

$$\varphi_1 = \frac{Q_i}{4\pi \varepsilon_0 L} \left(\frac{1}{2\pi} \sum_{\mathbf{n}>0} \frac{1}{n^2} \exp\left(-\frac{\pi^2 n^2}{\delta^2}\right) - \frac{\delta}{\sqrt{\pi}} \right) \tag{2}$$

and the binary contribution can be written as follows [2, 5]:

$$\varphi_2(\mathbf{r}_{ij}) = \frac{Q_j}{4\pi\varepsilon_0} \left(\frac{\mathrm{erfc}\left(\delta\frac{r_{ij}}{L}\right)}{r_{ij}} + \frac{1}{\pi L}\sum_{\mathbf{n}>0}\frac{1}{n^2}\exp\left(-\frac{\pi^2 n^2}{\delta^2}\right)\cos\left(\frac{2\pi}{L}\mathbf{n}\cdot\mathbf{r}_{ij}\right) \right). \tag{3}$$

Here δ/L is the conventional Ewald parameter [2], $\mathbf{n}/L$ is the three-dimensional reciprocal lattice site vector ($n = |\mathbf{n}|$) and $\mathrm{erfc}(x)$ is the complementary error function. Keeping in mind that all orientations of the main cell in an isotropic media should be equivalent, we can average both sides of equation (3) over all directions of the vector $\mathbf{n}$ at a fixed distance r_{ij}. Using brackets

$$\langle\cdots\rangle = \frac{1}{4\pi}\int_{-1}^{+1}\mathrm{d}(\cos\vartheta)\int_{-\pi}^{\pi}\mathrm{d}\psi\cdots,$$

where ψ, ϑ are the polar and azimuthal angles defining the direction of the vector $\mathbf{n}$ ($\mathbf{n}\cdot\mathbf{r} = nr\cos\vartheta$) to indicate such averaging, we can determine the pre-averaged (effective) potential as $\varphi_2(r_{ij}) \equiv \langle\varphi_2(\mathbf{r}_{ij})\rangle$. Integration of equation (3) over all orientations of the vector $\mathbf{n}$ gives immediately

$$\varphi_2(r_{ij}) = \frac{Q_j}{4\pi\varepsilon_0 r_{ij}}\left(\mathrm{erfc}\left(\delta\frac{r_{ij}}{L}\right) + \frac{1}{2\pi^2}\sum_{\mathbf{n}>0}\frac{1}{n^3}\exp\left(-\frac{\pi^2 n^2}{\delta^2}\right)\sin\left(\frac{2\pi}{L}nr_{ij}\right) \right). \tag{4}$$

The pre-averaged charge–charge potential, equation (4), is a continuous function of the inter-particle distance r_{ij} and can be expanded in converging power series in terms of this distance. Since both $\mathrm{erfc}(x) - 1$ and $\sin(x)$ are odd functions

$$\varphi_2(r_{ij}) = \frac{Q_j}{4\pi\varepsilon_0 r_{ij}}\left(1 + \sum_{k\geqslant 0}C_k r_{ij}^{2k+1} \right). \tag{5}$$

The coefficients C_k in equation (5) are found in [6] by direct expansion of equation (4) in a MacLaurin series. The procedure is straightforward: by applying the Euler–MacLaurin formula generalized for summation over three-dimensional integers $\mathbf{n}$ the following result holds [6]:

$$C_0 = \frac{1}{\pi}\sum_{\mathbf{n}>0}\frac{1}{n^2}\exp\left(-\frac{\pi^2 n^2}{\delta^2}\right) - \frac{2\delta}{\sqrt{\pi}}, \qquad C_1 = \frac{2\pi}{3L^3}, \qquad C_k = 0, \quad k > 1.$$

By taking into account the electroneutrality condition, equation (1), it can be seen that the term in equation (5) which is independent of distance (proportional to C_0) and the one-particle contribution, equation (2), cancel one another. This implies that the total Coulomb energy of N charged particles in the main cell can be described by the sum

$$U_N^{(C)} = -\sum_{i=1}^{N}\frac{3Q_i^2}{16\pi\varepsilon_0 r_m} + \frac{1}{2}\sum_{i=1}^{N}\sum_{j=1,j\neq i}^{N}\tilde{\phi}(r_{ij}), \tag{6}$$

where $\tilde{\phi}(r_{ij})$ is an effective potential defined by

$$\tilde{\phi}(r) = \begin{cases} \dfrac{Q_i Q_j}{4\pi\varepsilon_0 r}\left\{1 + \dfrac{1}{2}\left(\dfrac{r}{r_m}\right)\left[\left(\dfrac{r}{r_m}\right)^2 - 3\right]\right\} & r < r_m \\ 0 & r \geqslant r_m \end{cases} \tag{7}$$

and r_m is the radius of the volume-equivalent sphere $\left(\frac{4}{3}\pi r_m^3 = L^3\right)$ of the main cell.

Table 1. Comparison of predicted MC internal energies $-U_{\mathrm{MC}}^{(\mathrm{OCP})}/Nk_BT$ for OCP.

Γ	$N = 64$ (this work)	$N = 216$ [11]	$N = 686$ [12]
1	0.599 ± 0.010	0.580	
10	7.895 ± 0.020	7.996	
50	43.073 ± 0.019	43.094	
100	87.555 ± 0.033	87.480	87.52[a]
160	141.00 ± 0.016	140.89	141.72
200	176.62 ± 0.012		176.77[b]

[a] Best fit value.
[b] Fluid initial conditions.

The pair effective (pre-averaged) potential, equation (7), has the following properties:

- At small r it tends to the pure Coulomb pair potential minus constant shift.
- It is zero at $r = r_m$ and remains zero at $r > r_m$.
- Its first derivative is zero at $r = r_m$.
- Its range corresponds to the size of the main cell: $r_m = \left(\frac{3}{4\pi}\right)^{\frac{1}{3}} L = 0.620\,35L$.

The last property entails some inconsistency with the initial main cell configuration. If the range of interaction does not exceed $L/2$ each particle in the cell contributes (or not) to the sum of interactions with the selected one just once: either as the original object (inside the main cell) or as one of its 'images'. This is not the case for potential equation (7) because $r_m > L/2$. The subsequent modification of the simulation algorithm is formulated in [6]. Two different zones exist within the effective sphere surrounding an arbitrary charge in the main cell [6]. The first zone contains charged particles (inside the main cell) or their images (outside it) that contribute to the sum of pair interactions of the chosen charge just one time. The second zone contains those charged particles which contribute twice to the interaction energy with the given charge—both as original charges and as their additional 'phantom' images [6].

3. Applications to simplest plasma models

3.1. One-component plasma: MC simulation

The one-component plasma (OCP), i.e. a system of point ions placed in a rigid neutralizing background, is a text-book example of a classical Coulomb system for which the standard Ewald approach was successfully applied [11, 12]. Separating the interactions of the negative (background) charge distribution in equation (6) and replacing summation over negative ions by integration over uniformly distributed background charge, one gets the following generalization of equation (6) for the OCP:

$$U_N^{(\mathrm{OCP})} = -0.9\frac{N^2 Q^2}{4\pi \varepsilon_0 r_m} + \frac{1}{2}\sum_{i=1}^{N}\sum_{j=1, j\neq i}^{N} \tilde{\phi}(r_{ij}), \tag{8}$$

where N is the number of positive ions. It should be noted that both terms here are size dependent but not directly proportional to N. The first contribution in equation (8) per one ion at given temperature T can be expressed in terms of plasma parameter $\Gamma = Q^2 N^{1/3}(4\pi\varepsilon_0 r_m k_B T)^{-1}$ as $-0.9k_B T\Gamma N^{2/3}$. Two series of MC simulations using the method outlined above and the algorithm described in [6] were performed to prove that equation (8) gives correct estimations of the OCP energy at relatively small N and the mean value of $U_N^{(\mathrm{OCP})}/N$ converges at large N. Details of the MC simulation procedure were reported earlier [13, 14]. Results are presented in table 1 for $\Gamma = 1, \ldots, 200$ at fixed $N = 64$ and
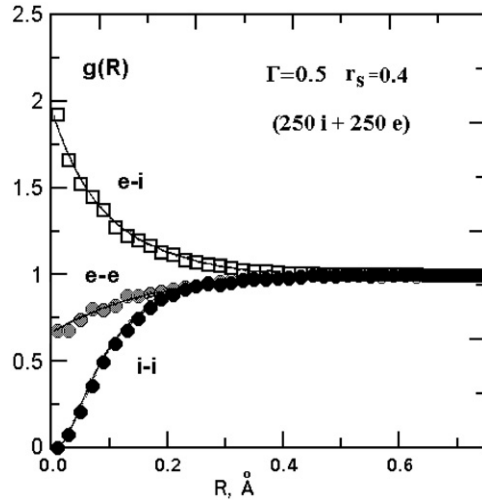
Figure 1. Thermal contribution $\Delta E^{(\text{th})}/Nk_BT = (U_N^{(\text{MC})} - U_N^{(\text{BCC})})/Nk_BT$ to internal energy of OCP at $\Gamma = 100$ calculated with the proposed effective potential and $U_N^{(\text{BCC})}(N)$ from [17] (open circles) in comparison with the conventional Ewald scheme [11] (solid square) and [12] (solid triangle).

compared in figure 1 to the MC data of Hansen [11], and Stringfellow, DeWitt and Slattery [12] for a wide range of N at fixed $\Gamma = 100$.

3.2. MD simulation of hydrogen plasma

Another simple model system suitable for testing of the method is the two-component semi-classical model of hydrogen plasma. In order to test the effectiveness and accuracy of the method described above, it was incorporated in our MD simulation program, described earlier [14], and the original MD simulation of Hansen and McDonald [15] repeated. Following [15], a version of the Glauberman–Yukhnovskii [16] potential model for ion–electron plasma was applied:

$$\phi_{\alpha\beta}(r) = \frac{Z_\alpha Z_\beta e^2}{r}[1 - \exp(-r/\lambda_{\alpha\beta})].\qquad(9)$$

Here, $\lambda_{\alpha\beta}$ is the thermal de Broglie wavelength, $\alpha, \beta = i$ (ions), e (electrons):

$$\lambda_{\alpha\beta} = \frac{h(m_\alpha + m_\beta)}{(2\pi)^{3/2}(m_\alpha m_\beta k_B T)^{1/2}}.\qquad(10)$$

Simulations were carried out on the same Γ and r_s as in the original work of Hansen and McDonald [15]. Some results for the same cell size (125 ions and 125 electrons) as used in [15] and a bigger cell size are presented in table 2 and figure 2. One can find details of the MD simulation procedure in [14]. In table 2, along with the compressibility factor and diffusion coefficients, the mean potential energy U and its configuration part U_{conf} are presented to illustrate the effect of temperature dependence on potential parameters $\lambda_{\alpha\beta}$ (equation (10)). It ought to be mentioned that the calculated PV/Nk_BT value deviates noticeably from that of [15] and it is not clear which one is correct. Hopefully MC simulations in the future development of this work will clarify this point.

4. Concluding remarks

Pre-averaging the Ewald sums over all spatial directions leads to an approach which eliminates periodicity artefacts imposed by the conventional Ewald scheme and provides a fast method

Figure 2. Radial distribution functions in hydrogen plasma. Comparison of our MD simulation results with the solutions of HNC integral equations [15] (solid lines).

Table 2. MD simulation of hydrogen plasma at $\Gamma = 2, r_s = 1$. Comparison with Hansen and McDonald [15]. Diffusion coefficients D_e and D_i are in 10^{-5} cm^2 s^{-1}.

	125i + 125e [15]	125i + 125e (this work)	250i + 250e (this work)
PV/Nk_BT	0.63	0.77	0.75
U_{conf}/Nk_BT	–	−1.12	−1.13
U/Nk_BT	–	−1.55	−1.51
D_e	2.47	2.83	2.78
D_i	0.047	0.048	0.049

for computation of the electrostatic contribution to the energy of disordered dense systems in MC or MD computer simulations [6].

All our simulations took from a few seconds up to a few hours per run on a PC depending on the size of the main cell. The performance of modern PCs when combined with the proposed method allows conventional MC/MD simulations to be run on cells containing up to several thousand charged particles.

This method was applied recently to several simple ordered structures [17]. It was found that the pre-averaging, originally devised for spatially uniform systems, provides surprisingly fast convergence of predicted energy to exact values in ordered crystalline NaCl, CsCl, OCP–BCC and CaF$_2$ structures despite the inevitable non-zero net charge inside the equivalent sphere. This makes feasible accurate simulations of Coulomb systems with large numbers of particles in the cell near the melting/crystallization point. New MC and MD results presented in section 3 prove the ability of the method to produce accurate results at low computational cost.

MC simulations of OCP (small cell size $N = 64$) presented in table 1 are in good agreement with other simulation data [11, 12]. At the same time the comparison presented in figure 1 shows that it is very likely coincidental. The convergence to a constant value at large N is non-monotonic. The thermal contribution to internal energy $\Delta E^{(\mathrm{th})}/Nk_BT$ at $\Gamma = 100$ shown in figure 1 is computed using values of E_{BCC}/Nk_BT calculated in [17] as a function of N. Our predictions are in reasonable agreement with Hansen [11] and Stringfellow, DeWitt

and Slattery [12]. A small (about 0.5% of the total energy) deviation from [12] is nevertheless well beyond the total estimated error of both simulations and requires additional study. This discrepancy might affect the location of the crystallization point in OCP and may be due to periodicity artefacts.

The last line in table 1 also ought to be commented on. OCP at $\Gamma = 200$ corresponds to an equilibrium BCC crystal [12] at large N. However, the small number of ions ($N = 64$) is incompatible with the formation of either BCC or FCC structures in the cell and corresponds in our simulation to the fluid state. When the cell is large enough ($N > 200$), OCP with the proposed effective potential crystallizes at $\Gamma > \Gamma_{cr}$ in the BCC lattice. The value of Γ_{cr} is about 180 and depends on N. In some range of Γ near Γ_{cr} both BCC and fluid structures (one metastable) exist.

Whether OCP comes to a 'glass transition' is an interesting problem raised recently by Daligault and Murillo [18]. According to our simulations, after fast cooling from the fluid (low Γ) state, OCP with proposed effective potential forms long-lived 'frozen structures' having energies higher than the equilibrium perfect BCC crystalline OCP. Ions in these structures, in contrast to the conventional 'glassy state', are locally spatially ordered. Direct visualization clearly reveals their highly imperfect polycrystalline structure with a certain amount of relatively stable defects (dislocations, etc) which long after, eventually disappear.

To conclude, it ought to be mentioned that the technique proposed is applicable for quantum Coulomb systems as well as for Coulomb systems with arbitrary short-range interaction in frames of different *ab initio* approaches such as path integral Monte Carlo, etc, and may be combined with density functional theory. The method may be used as an effective tool in simulations of high-energy density matter produced by ultrafast proton beams [20] or hadron colliders [19]. We believe that the implementation of pre-averaged potentials in existing and upcoming computer simulation packages may essentially speed up conventional MC and MD simulations of strongly coupled Coulomb systems and decrease errors caused by periodicity artefacts in *ab initio* computer simulations with small numbers of particles in the main cell, especially near the phase transition points.

References

[1] Madelung E 1918 *Phys. Z.* **19** 524
[2] Ewald P P 1921 *Ann. Phys., Lpz.* **64** 253
[3] Hockney R W and Eastwood J W 1981 *Computer Simulation Using Particles* (New York: McGraw-Hill)
[4] Car R and Parrinello M 1985 *Phys. Rev. Lett.* **55** 2471
[5] Rappaport D C 1995 *The Art of Molecular Dynamics Simulation* (Cambridge: Cambridge University Press)
[6] Yakub E S and Ronchi C 2003 *J. Chem. Phys.* **119** 11556
[7] Bonev S A, Militzer B and Galli G 2004 *Phys. Rev.* B **69** 014101 and references therein
[8] Gygi F 2003 *Ab Initio Molecular Dynamics Code* GP 1.20.0 (Lawrence Livermore National Laboratory)
[9] Andreoni W and Curioni A 2000 *Parallel Comput.* **26** 819
[10] Ding H-Q, Karasawa N and Goddard W A 1992 *J. Chem. Phys.* **97** 4309
[11] Hansen J P 1973 *Phys. Rev.* A **8** 3110
[12] Stringfellow G S, DeWitt H E and Slattery W L 1990 *Phys. Rev.* A **41** 1105
[13] Yakub E S 2001 *J. Low Temp. Phys.* **122** 559
[14] Yakub E S 2001 *J. Mol. Liq.* **93** 69
[15] Hansen J P and McDonald I R 1981 *Phys. Rev.* A **23** 2041
[16] Glauberman A E and Yukhnovskii I R 1953 *Dokl. Akad. Nauk SSSR* **93** 999
[17] Yakub E S and Ronchi C 2005 *J. Low Temp. Phys.* **139** 633
[18] Daligault J O and Murillo M S 2005 *Int. Conf. on Strongly Coupled Coulomb Systems (Moscow, 20–25 June)* Book of Abstracts vol 32
[19] Patel P K *et al* 2003 *Phys. Rev. Lett.* **91** 125004
[20] Tahir N A *et al* 2005 *Phys. Rev. Lett.* **94** 135004